

Cite this: *Chem. Sci.*, 2012, **3**, 2457

www.rsc.org/chemicalscience

EDGE ARTICLE

Photochemical tyrosine oxidation with a hydrogen-bonded proton acceptor by bidirectional proton-coupled electron transfer†

Arturo A. Pizano, Jay L. Yang and Daniel G. Nocera*

Received 26th January 2012, Accepted 14th May 2012

DOI: 10.1039/c2sc20113e

Amino acid radical generation and transport are fundamentally important to numerous essential biological processes to which small molecule models lend valuable mechanistic insights. Pyridyl-amino acid-methyl esters are appended to a rhenium(i) tricarbonyl 1,10-phenanthroline core to yield rhenium-amino acid complexes with tyrosine ([Re]-Y-OH) and phenylalanine ([Re]-F). The emission from the [Re] center is more significantly quenched for [Re]-Y-OH upon addition of base. Time-resolved studies establish that excited-state quenching occurs by a combination of static and dynamic mechanisms. The degree of quenching depends on the strength of the base, consistent with a proton-coupled electron transfer (PCET) quenching mechanism. Comparative studies of [Re]-Y-OH and [Re]-F enable a detailed mechanistic analysis of a bidirectional PCET process.

Introduction

Tyrosyl radicals are key intermediates in a wide variety of bio-energy conversion processes.¹ The proton-coupled electron transfer (PCET) component of tyrosine oxidation has been of particular interest both in natural² and model systems.^{3,4} Tyrosyl radicals are essential to a biology as diverse as that derived from photosystem II,^{5,6} cytochrome *c* oxidase⁷ and ribonucleotide reductase (RNR).⁸ We have developed biophysical tools that permit tyrosine radicals (Y·) to be photogenerated in biological systems with emphasis on RNR.⁹ These photoRNRs have been invaluable for deciphering the PCET mechanism by which radicals are generated and transported in this enzyme.^{10–13} The value of Y· photogeneration in the development of new biophysical tools for radical enzymology¹⁴ provides an imperative for a mechanistic understanding of tyrosine photooxidation.

Formation of tyrosyl radical from tyrosine requires both deprotonation and one-electron oxidation of the native amino acid. Stepwise mechanisms are thermodynamically demanding and result in high-energy intermediates, implicating a PCET mechanism for this reaction. In natural systems, PCET processes occur with exquisite sensitivity and remarkable selectivity by separating the PT coordinate from the ET coordinate, *i.e.* by installing a bidirectional PCET pathway. This requirement is due to the relatively large mass of a proton in comparison to an electron. Hence, whereas the electron can tunnel over long

distances, the proton cannot,^{15,16} as such, the control of the PT coordinate over a different length scale to that of the electron is essential for the kinetic feasibility of a PCET reaction and the attendant opportunity to exercise kinetic control over the reaction.

To this end, well-defined, pre-organized PT pathways that incorporate a proton acceptor are essential for the generation of Y·. A variety of studies have demonstrated the importance of hydrogen bonding on the kinetics of phenol oxidation by PCET.^{17–22} Herein, we report the use of a bidirectional scaffold for the study of tyrosine oxidation that enables the independent variation of the driving force for both proton transfer (PT) and electron transfer (ET), which are critical determinants of the PCET governing tyrosine photooxidation.²³ A pyridyl-amino acid-methyl ester (Py-AA) has been appended to a rhenium(i) tricarbonyl 1,10-phenanthroline core [Re] to yield rhenium-amino acid complexes with tyrosine ([Re]-Y-OH) and phenylalanine ([Re]-F). A PCET network is self assembled by association of [Re]-Y-OH to a base, which is both well-defined and easily varied to permit the PT to be examined in concert with ET to the photoexcited [Re] core. We find that the efficacy of radical generation depends intimately on the strength of the associated base.

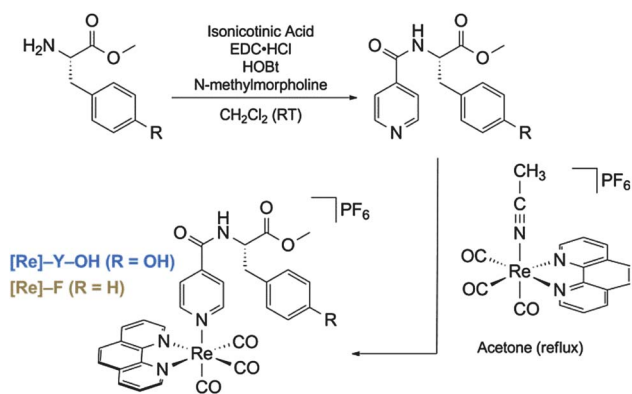
Experimental

The [Re]-AA compounds are synthesized *via* the route shown in Scheme 1. Syntheses were accomplished by methodologies described in the ESI† and products were spectroscopically and analytically characterized in detail to ensure compound identification and purity; these data are also given in the ESI†.

Steady-state spectroscopy was performed using dilute solutions of [Re]-AA (AA = Y or F) complexes. Emission titrations

Department of Chemistry, Massachusetts Institute of Technology, 77 Massachusetts Avenue, Cambridge, MA, 02139-4307, USA. E-mail: nocera@mit.edu; Tel: +617 253 5537

† Electronic supplementary information (ESI) available: Synthetic procedures, detailed experimental methods, kinetic analysis, fitting details, base concentration-dependent emission quenching data. See DOI: 10.1039/c2sc20113e



Scheme 1

were performed by adding sequential volumes of pyridine (neat) or imidazole (1.0 M in dichloromethane) to a sample of [Re]-Y-OH (50 μ M in dichloromethane). Equilibrium constants were determined for the association of [Re]-Y-OH and pyridine or imidazole by monitoring emission quenching as a function of base added. Fitting to determine the equilibrium association constants for [Re]-Y-OH binding to bases was performed according to published methods.²⁴

Time-resolved absorption and emission experiments were completed by nanosecond flash photolysis, which were performed using a system which was significantly modified from one previously described.^{25,11} Emission lifetimes were measured for both [Re]-Y-OH and [Re]-F as a function of pyridine and imidazole concentrations. Full experimental procedures, detailed description of experimental apparatus, a complete explanation of data analysis, and a derivation of the rate law for excited-state quenching are provided in ESI†. Errors reported for rate constants and equilibrium constants measured are two standard deviations, as calculated from the standard error of the corresponding fit.

Results and discussion

The [Re]-AA compounds shown in Scheme 1 were developed as a modular platform where relevant driving forces could be varied for the study of PCET. A similar method of their synthesis has recently been reported.²⁶ The PCET network is self assembled by addition of base (pyridine or imidazole) to a solution of [Re]-Y-OH in dichloromethane as shown in Fig. 1. This approach for forming the bidirectional PCET network provides a modular and versatile platform for studying tyrosine oxidation. The absence of a hydrogen bond in the

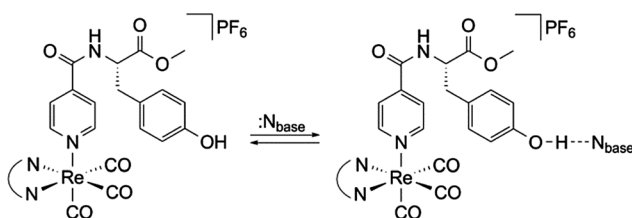


Fig. 1 Self-assembly of a bidirectional network for the photooxidation of tyrosine by PCET.

[Re]-F system prevents assembly of the PCET network, and hence this system provides a control for kinetic measurements associated with the photogeneration of $Y\cdot$. Moreover, because F is redox inactive, any disparity in excited-state lifetimes between [Re]-F and [Re]-Y-OH is directly attributable to reactivity at the tyrosine phenol.

Ground-state absorption and steady-state emission spectra of [Re]-Y-OH and [Re]-F (Fig. 2) are nearly identical to one another and dominated by the electronic properties of the [Re] centre. Hydrogen-bonded association between the tyrosine phenol proton of [Re]-Y-OH and base is evident from emission spectra. In dichloromethane solution, [Re]-Y-OH is highly emissive from a ³MLCT excited state (³[Re]^I*). As shown in Fig. 3, emission from [Re]-Y-OH is quenched significantly upon addition of base (pyridine or imidazole). The equilibrium constants, K_{assoc} , for association between [Re]-Y-OH and the added base may be determined from the concentration dependence of this quenching. Equilibrium constants were measured for both pyridine ($K_{\text{assoc}} = 16 \pm 2 \text{ M}^{-1}$) and imidazole ($K_{\text{assoc}} = 157 \pm 13 \text{ M}^{-1}$) by fitting the concentration dependence of emission intensity as previously reported.²⁴ These equilibrium constants correspond to reaction free energies of $\Delta G^\circ = -6.9 \text{ kJ mol}^{-1}$ and $\Delta G^\circ = -12.5 \text{ kJ mol}^{-1}$. The stronger binding to imidazole than to pyridine is in accordance with the relative aqueous pK_a values of the bases.

Transient absorption spectra indicate that the ³[Re]^I* excited state reacts with base by electron transfer. The transient absorption spectra and single-wavelength kinetic data for solutions of [Re]-Y-OH and [Re]-F in dichloromethane are shown in Fig. 4 (top) in the absence of base. Transient spectra exhibit absorption features as expected for compounds of this type.²⁷ Significant growth features are observed at 300 and 450 nm. The transient signals decay monoexponentially; the lifetime of the ³[Re]^I* excited state in [Re]-Y-OH is slightly shorter than for [Re]-F. This is consistent with oxidation of tyrosine by [Re]-Y-OH. The ³[Re]^I* excited state is highly oxidizing and is of sufficient potential to oxidize the base ($E^\circ(\text{Re}^{\text{I}/0}) = 1.7 \text{ V vs. NHE}$).²⁸ The given value was measured in acetonitrile and provides only an estimate for the present report where experiments are conducted in dichloromethane.

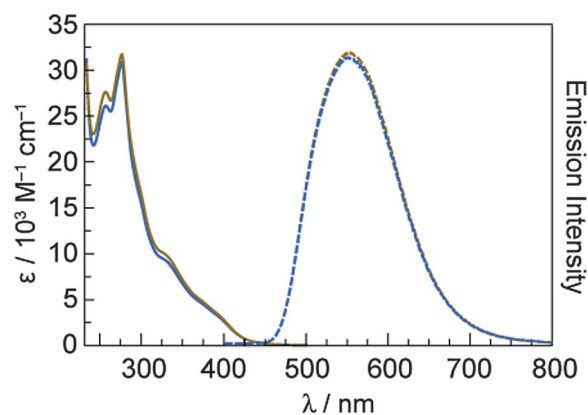


Fig. 2 Electronic absorption (solid lines) and emission ($\lambda_{\text{exc}} = 355 \text{ nm}$) (dashed lines) spectra of [Re]-Y-OH (gold) and [Re]-F (blue) at 50 μ M concentration in dichloromethane.

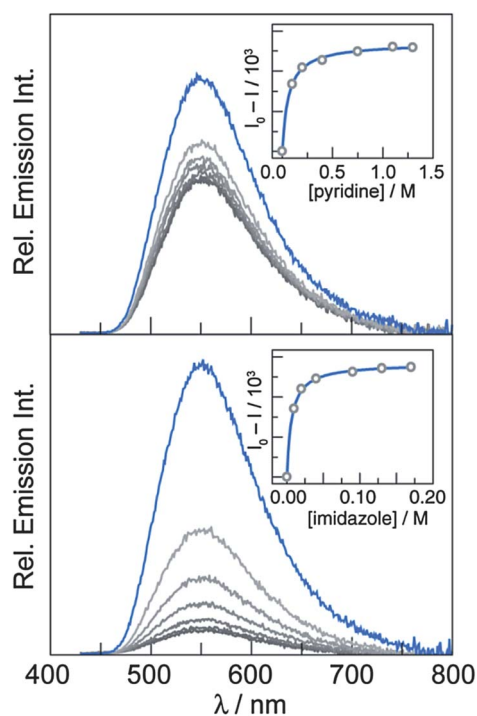


Fig. 3 Excited-state quenching titrations monitored by steady-state emission of [Re]-Y-OH. Addition of pyridine (top) or imidazole (bottom) to solutions of [Re]-Y-OH (50 μM in dichloromethane) results in significant quenching of steady-state emission ($\lambda_{\text{exc}} = 400 \text{ nm}$). Spectra are shown in the absence of base (blue) and the presence of increasing concentrations of base (grey). Association constants are calculated using integrated emission intensity as previously reported (insets).²⁴

Furthermore, previously reported electrochemical experiments show the onset of pyridine and imidazole oxidation at potentials of $\sim 1.6 \text{ V}^{29}$ and $\sim 1.4 \text{ V}^{30}$ vs. NHE, respectively. These values are consistent with oxidation by the $^3[\text{Re}^{\text{I}}]^*$ excited state as well as the relative rates of oxidation for imidazole and pyridine.

When pyridine or imidazole is added to solutions of [Re]-F and [Re]-Y-OH, the TA signal of the $^3[\text{Re}^{\text{I}}]^*$ excited state is considerably shortened, more so for imidazole than pyridine (Fig. 4, bottom). Concentrations of base were chosen to ensure that at least 95% of [Re]-Y-OH was bound. We note that a transient signal for photooxidized tyrosine is not observed, indicating that the intermediate does not accumulate owing to back electron transfer rate that is faster than the forward PCET rate for quenching.

In the absence of direct observation of a transient absorption signal owing to a fast back reaction, the excited-state kinetics were further examined by transient emission spectroscopy. The quenching paths of $^3[\text{Re}^{\text{I}}]^*$ for [Re]-F and [Re]-Y-OH are shown in Fig. 5. In this model, we assume that the intrinsic decay processes and bimolecular processes of [Re]-Y-OH and [Re]-Y-OH $\cdots\text{N}_{\text{base}}$ are similar.

The excited-state reactivity of [Re]-F with base is straightforward; the emission will decay with intrinsic radiative and nonradiative process defined by $k_0 (= 1/\tau_0)$ or react with base by electron transfer, defined by the bimolecular quenching rate constant k_q . In a Stern-Volmer process, the overall observed

emission rate constant for reaction ($= 1/\tau_{\text{F}}$) should follow the kinetics,

$$k_{\text{obs}} = 1/\tau_{\text{F}} = k_0 + k_q[\text{base}] \quad (1)$$

As predicted by eqn (1), Stern-Volmer plots are linear with increasing concentration of base. From the natural lifetime of $^3[\text{Re}^{\text{I}}]^*$ in Fig. 4, bimolecular quenching rate constants $k_q = 3.2(6) \times 10^5 \text{ M}^{-1} \text{ s}^{-1}$ and $3.1(6) \times 10^7 \text{ M}^{-1} \text{ s}^{-1}$ for pyridine and imidazole, respectively. These data are summarized in Table 1.

The excited-state decay processes of $^3[\text{Re}^{\text{I}}]^*$ in the [Re]-Y-OH $\cdots\text{N}_{\text{base}}$ assembly are richer. In addition to the natural decay of the $^3[\text{Re}^{\text{I}}]^*$ excited state and its bimolecular quenching by base, two unique unimolecular processes arise from electron transfer from Y-OH to $^3[\text{Re}^{\text{I}}]^*$ and from PCET. The excited-state dynamics of the rhenium center should not be affected by the remote amino acid inasmuch as it is not conjugated to the ligands of the rhenium center. Hence k_0 and k_q , to a first approximation, should be the same for both systems. One possible exception to this approximation may be the difference in reduction potential of the bound base relative to base in solution; however, the large excess of free base is expected to dominate the kinetics of base-oxidation by $^3[\text{Re}^{\text{I}}]^*$. Moreover, lacking the tyrosine phenol, Re-F cannot be oxidized by $^3[\text{Re}^{\text{I}}]^*$; oxidation of toluene (a suitable approximation to the phenylalanine sidechain) occurs at a potential greater than that of $^3[\text{Re}^{\text{I}}]^*$ (1.8 V³¹ vs. NHE). Accordingly, the Re-F center provides a reference for the ET process between the unassociated tyrosine and the excited rhenium center.

The k_{ET} rate constant is given by,

$$k_{\text{ET}} = \frac{1}{\tau_{\text{obs}}} - \frac{1}{\tau_0} \quad (2)$$

From the data in Fig. 4 and rate constants summarized in Table 1, a $k_{\text{ET}} = 6.1 \times 10^4 \text{ s}^{-1}$ is determined. Whereas the kinetics associated with ET are straightforward, the PCET process is more complicated. The emission decay dynamics are modulated by the equilibrium between [Re]-Y-OH and N_{base} . For this reason, a linear Stern-Volmer relation is not expected. Indeed, the base concentration dependence of the emission lifetime exhibits significant curvature as shown in Fig. S1 (ESI \dagger). The rate of excited-state decay for [Re]-Y-OH varies as a function of base concentration according to eqn (3),

$$k_{\text{obs}} = \frac{1}{\tau_{\text{Y}}} = k_0 + k_q[\text{base}] + k_{\text{ET}} + k_{\text{PCET}} \frac{K_{\text{assoc}}[\text{base}]}{1 + K_{\text{assoc}}[\text{base}]} \quad (3)$$

Detailed derivations of rate laws are available in the ESI \dagger . The last term of the above equation accounts for the equilibrium between [Re]-Y-OH and base, and the PCET process enabled by that equilibrium. Although variations in the observed rate constants (k_0 , k_{ET} , k_q) may occur as a result of hydrogen bonding to the tyrosine phenol, in the context of the final analysis, where the PCET rates exceed k_{ET} by a factor of 10 or 100, variation in k_{ET} is unlikely to cause significant interference with the calculation of k_{PCET} . The only unknown variable in the above equation is k_{PCET} . Fitting the observed rate constant for excited-state deactivation, k_{obs} (as calculated from the emission lifetime), to the concentration of base furnishes $k_{\text{PCET}} = 4.1(6) \times 10^5 \text{ s}^{-1}$ and $k_{\text{PCET}} = 4.8(8) \times 10^6 \text{ s}^{-1}$ for pyridine and imidazole, respectively.

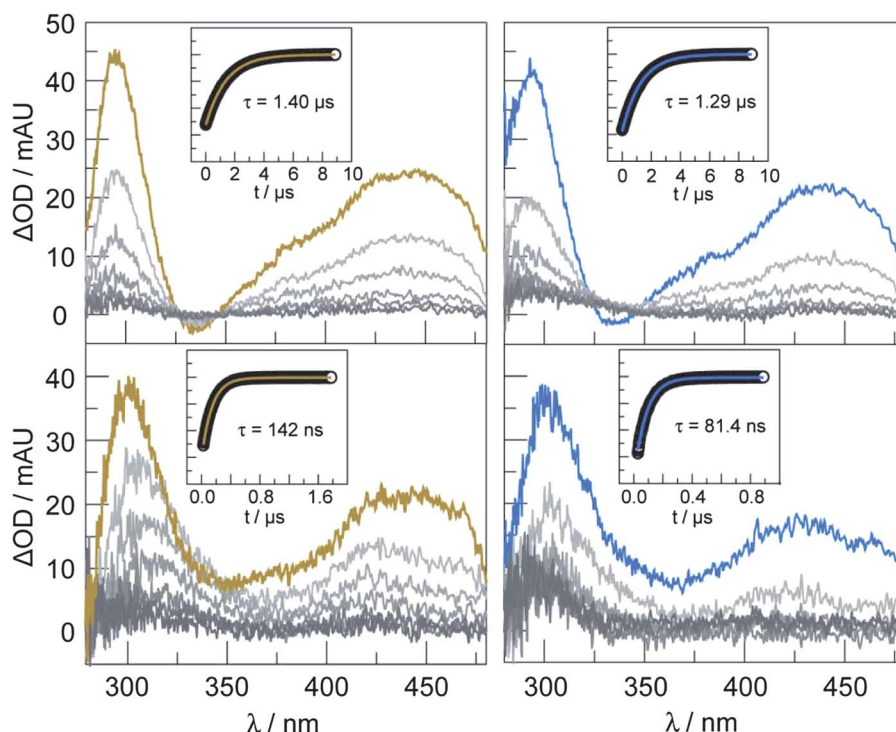


Fig. 4 Transient absorption spectra ($\lambda_{\text{exc}} = 355 \text{ nm}$) of [Re]-F (gold) and [Re]-Y-OH (blue) ($50 \mu\text{M}$ in dichloromethane) in the absence of base (top) and in the presence of 0.20 M imidazole (bottom). Spectra are collected immediately after the laser pulse and every 1000 ns (in the absence of base) or 150 ns (in the presence of base) thereafter (shown in grey). Single-wavelength emission decay kinetics monitored at 550 nm are shown in the insets. Decays are monoexponential. The lifetimes derived from the monoexponential fit, shown by the solid line, are given.

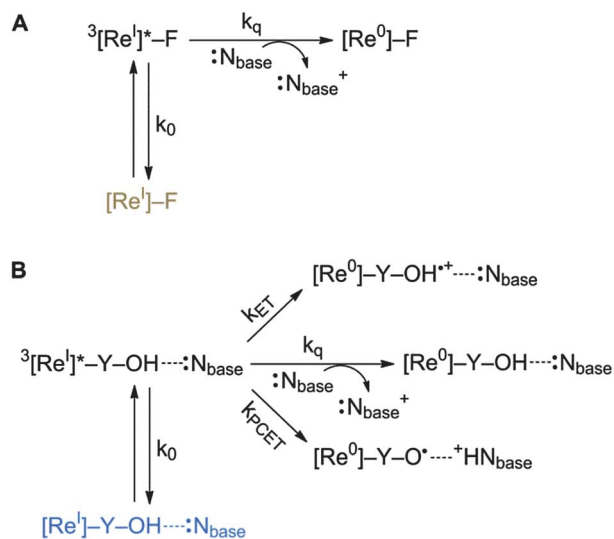


Fig. 5 Excited-state quenching pathways for (A) [Re]-F and (B) [Re]-Y-OH \cdots N_{base}. The rate constants k_0 and k_q are assumed to be the same for both paths (A) and (B), and are defined by the natural lifetime of [Re]-F and the quenching of [Re]-F by base, respectively.

These PCET rates are comparable to those previously observed in unimolecular systems incorporating hydrogen bonding to phenols within bimolecular¹⁷ and unimolecular (tethered)¹⁸ frameworks. In these cases, the photoacceptor is ruthenium(II) tris(bipyridine), which is less oxidizing than Re(I) polypyridyl excited states. Hydrogen bonding facilitates PCET

Table 1 Values for rate constants shown in Fig. 5 for excited state dynamics of [Re]-F and [Re]-Y-OH associated to base

Base independent parameters		
	[Re]-F	[Re]-Y-OH
k_0^a/s^{-1}	7.1×10^5	7.1×10^5
$k_{\text{ET}}^b/\text{s}^{-1}$	—	6.1×10^4
Base association and related kinetic parameters		
	Pyridine	Imidazole
$k_q^c/\text{M}^{-1} \text{ s}^{-1}$	$3.2(6) \times 10^5$	$3.1(6) \times 10^7$
$K_{\text{assoc}}/\text{M}^{-1}$	16(2)	157(13)
$k_{\text{PCET}}/\text{s}^{-1}$	$4.1(6) \times 10^5$	$4.8(8) \times 10^6$

by substantially decreasing the inner-sphere contribution to reorganization energy from the phenol and by introducing ‘promoting’ vibrational modes; the thermodynamic strength of the hydrogen bond has been observed to have a lesser impact on PCET rate enhancement.¹⁹ This is not the case here. The rate-enhancement for phenol oxidation in [Re]-Y-OH \cdots N_{base} varies with the strength of the hydrogen bond, as has also recently been observed in protein maquettes.³² The correlation may be more apparent for [Re]-Y-OH \cdots N_{base} owing to the similarity of the hydrogen bond type formed by imidazole and pyridine. Previous studies on phenol photooxidations have emphasized hydrogen bonding networks that are formed from carboxylates where differences in the hydrogen-bonded adduct (e.g., six- or

seven-membered rings formed in the two cases) likely introduce important vibrational effects and greater sensitivity to the vibrational modes of the hydrogen-bonding network. When this complexity is removed, it appears that the PCET rate for photooxidation follows a more straightforward thermodynamic trend with the strength of the hydrogen bonds within the PCET network.

With respect to the observed variation of k_{PCET} with the proton acceptor pK_{a} , previous work in a bimolecular system has shown that as the strength of the base (proton acceptor) increases, faster rates of PCET are observed for phenol oxidation.^{33,34} In recent related work, the importance of hydrogen bond distance (rather than strength) on the rate of PCET reactions has been investigated.^{35,36} Although the present scaffold does not offer a way to directly control the proton transfer distance, the facile variation of hydrogen-bond strength that can be achieved with this scaffold may yield valuable insights of interest to this discussion.

Conclusions

The supramolecular assembly formed between a rhenium–tyrosine complex associated to base establishes a network for the photogeneration of tyrosyl radical by a PCET mechanism. An equilibrium interaction between the tyrosine phenol proton and bases in solution provides a well-defined proton acceptor network, simplifying analysis of PCET kinetics. The observed rates of tyrosine oxidation associated to base are consistent with those reported in the literature for intramolecular model systems. The approach affords for the self-assembly of a modular scaffold for the study of bidirectional PCET by simply varying the nature of the base. To this end, the approach reduces the complexity associated with the synthesis of tethered networks.

Acknowledgements

We wish to thank Dr Emily J. McLaurin for assistance with preliminary laser flash photolysis experiments. This research was supported by the National Institutes of Health (GM47274).

Notes and References

- 1 L. Hammarström and S. Styring, *Energy Environ. Sci.*, 2011, **4**, 2379.
- 2 D. L. Jenson and B. A. Barry, *J. Am. Chem. Soc.*, 2009, **131**, 10567.
- 3 H. Ishikita, A. V. Soudackov and S. Hammes-Schiffer, *J. Am. Chem. Soc.*, 2007, **129**, 11146.
- 4 T. Irebo, S. Y. Reece, M. Sjödin, D. G. Nocera and L. Hammarström, *J. Am. Chem. Soc.*, 2007, **129**, 15462.

- 5 J. M. Keough, D. L. Jenson, A. N. Zuniga and B. A. Barry, *J. Am. Chem. Soc.*, 2011, **133**, 11084.
- 6 B. A. Barry, *J. Photochem. Photobiol., B*, 2011, **104**, 60.
- 7 V. R. I. Kaila, M. I. Verkhovskiy and M. Wikström, *Chem. Rev.*, 2010, **110**, 7062.
- 8 J. Stubbe, D. G. Nocera, C. S. Yee and M. C. Y. Chang, *Chem. Rev.*, 2003, **103**, 2167.
- 9 S. Y. Reece, J. M. Hodgkiss, J. Stubbe and D. G. Nocera, *Philos. Trans. R. Soc. London, Ser. B*, 2006, **361**, 1351.
- 10 M. C. Y. Chang, C. S. Yee, J. Stubbe and D. G. Nocera, *Proc. Natl. Acad. Sci. U. S. A.*, 2004, **101**, 6882.
- 11 S. Y. Reece, M. R. Seyedsayamdost, J. Stubbe and D. G. Nocera, *J. Am. Chem. Soc.*, 2007, **129**, 13828.
- 12 P. G. Holder, A. A. Pizano, B. L. Anderson, J. Stubbe and D. G. Nocera, *J. Am. Chem. Soc.*, 2012, **134**, 1172.
- 13 A. A. Pizano, D. A. Lutterman, P. G. Holder, T. S. Teets, J. Stubbe and D. G. Nocera, *Proc. Natl. Acad. Sci. U. S. A.*, 2011, **109**, 39.
- 14 S. Y. Reece and D. G. Nocera, *Annu. Rev. Biochem.*, 2009, **78**, 673.
- 15 R. I. Cukier and D. G. Nocera, *Annu. Rev. Phys. Chem.*, 1998, **49**, 337.
- 16 S. Hammes-Schiffer, *Acc. Chem. Res.*, 2009, **42**, 1881.
- 17 M. Sjödin, T. Irebo, J. E. Utas, J. Lind, G. Merényi, B. Åkermark and L. Hammarström, *J. Am. Chem. Soc.*, 2006, **128**, 13076.
- 18 T. Irebo, O. Johansson and L. Hammarström, *J. Am. Chem. Soc.*, 2008, **130**, 9194.
- 19 L. O. Johannissen, T. Irebo, M. Sjödin, O. Johansson and L. Hammarström, *J. Phys. Chem. B*, 2009, **113**, 16214.
- 20 I. J. Rhile and J. M. Mayer, *J. Am. Chem. Soc.*, 2004, **126**, 12718.
- 21 I. J. Rhile, T. F. Markle, H. Nagao, A. G. DiPasquale, O. P. Lam, M. A. Lockwood, K. Rotter and J. M. Mayer, *J. Am. Chem. Soc.*, 2006, **128**, 6075.
- 22 T. F. Markle and J. M. Mayer, *Angew. Chem., Int. Ed.*, 2008, **47**, 738.
- 23 J. Bonin, C. Constantin, C. Louault, M. Robert, M. Routier and J.-M. Savéant, *Proc. Natl. Acad. Sci. U. S. A.*, 2010, **107**, 3367.
- 24 J. J. Concepcion, M. K. Brennaman, J. R. Deyton, N. V. Lebedeva, M. D. E. Forbes, J. M. Papanikolas and T. J. Meyer, *J. Am. Chem. Soc.*, 2007, **129**, 6968.
- 25 Z.-H. Loh, S. E. Miller, C. J. Chang, S. D. Carpenter and D. G. Nocera, *J. Phys. Chem. A*, 2002, **106**, 11700.
- 26 A. M. Blanco-Rodríguez, M. Towrie, J. Sýkora, S. Zálíš and A. Vlček, Jr., *Inorg. Chem.*, 2011, **50**, 6122.
- 27 K. Kalyanasundaram, *J. Chem. Soc., Faraday Trans.*, 1986, **82**, 2401.
- 28 D. M. Dattelbaum, K. M. Omberg, J. R. Schoonover, R. L. Martin and T. J. Meyer, *Inorg. Chem.*, 2002, **41**, 6071.
- 29 D. Aurbach and Y. Gofer, in *Nonaqueous Electrochemistry*, ed. D. Aurbach, CRC Press, Boca Raton, FL, 1999, pp. 137–212.
- 30 H. L. Wang, R. M. O'Malley and J. E. Fernandez, *Macromolecules*, 1994, **27**, 893.
- 31 L. F. D'Elia and R. L. Ortiz, *J. Electrochem. Soc.*, 2006, **153**, D187.
- 32 M. C. Martínez-Rivera, B. W. Berry, K. G. Valentine, K. Westerlund, S. Hay and C. Tommos, *J. Am. Chem. Soc.*, 2011, **133**, 17786.
- 33 C. J. Fecenko, T. J. Meyer and H. Thorp, *J. Am. Chem. Soc.*, 2006, **128**, 11020.
- 34 C. J. Fecenko, H. Thorp and T. J. Meyer, *J. Am. Chem. Soc.*, 2007, **129**, 15098.
- 35 T. F. Markle, I. J. Rhile and J. M. Mayer, *J. Am. Chem. Soc.*, 2011, **133**, 17341.
- 36 M.-T. Zhang, T. Irebo, O. Johansson and L. Hammarström, *J. Am. Chem. Soc.*, 2011, **133**, 13224.